Article

Measurement of C and N Isotopic Composition on Nanomolar Quantities of C and N

Pratigya J. Polissar, James M. Fulton, Christopher K. Junium, Courtney C. Turich, and Katherine H. Freeman

More About This Article

Additional resources and features associated with this article are available within the HTML version:

- Supporting Information
- Access to high resolution figures
- Links to articles and content related to this article
- Copyright permission to reproduce figures and/or text from this article

View the Full Text HTML

Measurement of ^{13}C and ^{15}N Isotopic Composition on Nanomolar Quantities of C and N

Pratigya J. Polissar,* James M. Fulton, Christopher K. Junium, Courtney C. Turich,[†] and Katherine H. Freeman

Department of Geosciences, The Pennsylvania State University, University Park, Pennsylvania 16802

We describe a trapping and chromatography system that cryogenically removes CO_2 and N_2 generated from sample combustion in an elemental analyzer (EA) and introduces these gases into a low-flow helium carrier stream for isotopic analysis. The sample size required for measurement by this system (termed nano-EA/IRMS) is almost 3 orders of magnitude less than conventional EA analyses and fills an important niche in the range of analytical isotopic methods. Only 25 nmol of N and 41 nmol of C are needed to achieve 1.0 ‰ precision (2σ) from a single measurement while larger samples and replicate measurements provide better precision. Analyses of standards demonstrate that nano-EA measurements are both accurate and precise, even on nanomolar quantities of C and N. Conventional and nano-EA measurements on international and laboratory standards are indistinguishable within analytical precision. Likewise, nano-EA values for international standards do not differ statistically from their consensus values. Both observations indicate the nano-EA measurements are comparable to conventional EA analyses and accurately reproduce the VPDB and AIR isotopic scales. Critical to the success of the nano-EA system is the procedure for removing the blank contribution to the measured values. Statistical treatment of uncertainties for this procedure yields an accurate method for calculating internal and external precision.

Isotopic abundances for C and N are typically determined on gaseous CO_2 and N_2 with a gas-source isotope-ratio mass spectrometer. These analyte gases are either produced from the sample material offline and introduced by a dual-inlet system or produced in a continuous-flow reactor system directly coupled to the mass spectrometer. Because most or all of the analyte gas is fed to the mass spectrometer source, continuous-flow systems can have dramatically lower sample size requirements than offline preparation. Continuous-flow analyses of the C and N isotopic composition of bulk organic materials are routinely accomplished using an elemental analyzer (EA) coupled to an isotope-ratio mass spectrometer (IRMS). Typi-

cally at least 2 μmol of C or N are required for these analyses.[1] Despite the utility of EA-IRMS, there are many situations where the available sample size is much less than required by this technique.

The sample size requirements for EA-IRMS are elevated in commercial systems because of the high split ratio of the carrier gas to the ion source. Elemental analyzers typically employ helium flow rates of 50−150 cm³ min⁻¹, yet only ∼0.2 cm³ min⁻¹ of this flow is transferred to the ion source of the IRMS. Although some adjustment can be made to increase the proportion of gas that flows into the ion source, in most instrument configurations, the lower limit on sample size is constrained by the minimum acceptable helium flow in the EA and the maximum flow rate that ion source pumps can accommodate. Ultimately the ionization efficiency of the MS and the relative abundance of the rare isotope control the minimum sample size required for acceptable analytical precision (determined by shot-noise statistics[2]).

Here we describe a system capable of analyzing the stable isotope composition of samples containing as little as ∼25−40 nM quantities of C and N. The system combines a modified commercially available combustion EA with a custom trapping and chromatography system that dramatically reduces sample size requirements. Sample gas (CO_2, N_2) from a high-flow EA effluent is cryogenically trapped and introduced into a low-flow helium stream (1−10 cm³ min⁻¹) that carries the sample gas to a capillary column where the gases are separated. The flow rate to the MS is maintained at 0.2 cm³ min⁻¹, as in the typical EA-IRMS configuration. This system significantly reduces the minimum sample size required for EA analysis by both increasing the height/width ratio of the analyte peak and decreasing the EA/IRMS split ratio from between 250:1−750:1 to as low as 5:1. The lower split ratio increases the peak area 50−150 times while the improved peak shape doubles the peak height. The net effect is a 100- to 500-fold decrease in sample size.

The principle for this system was first described by Fry et al.;[3] however, the current system differs in several key aspects including lower sample sizes in both C and N, excellent isotopic linearity, chromatographic separation and purification of analyte gases, and sequential measurements of C and N isotopes on single

* Corresponding author. E-mail: ppolissa@geosc.psu.edu. Fax: (814) 863-7823.
† Present address: ConocoPhillips, 600 N. Dairy Ashford, Houston, TX 77079.

(1) Werner, R. A.; Bruch, B. A.; Brand, W. A. *Rapid Commun. Mass Spectrom.* **1999**, *13*, 1237–1241.
(2) Merritt, D. A.; Hayes, J. M. *Anal. Chem.* **1994**, *66*, 2336–2347.
(3) Fry, B.; Garritt, R.; Tholke, K.; Neill, C.; Michener, R. H.; Mersch, F. J.; Brand, W. A. *Rapid Commun. Mass Spectrom.* **1996**, *10*, 953–958.
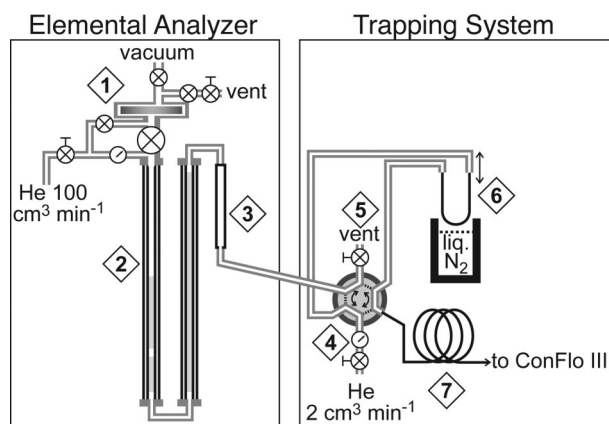
Figure 1. The nano-EA system includes an autosampler modified with a vacuum line and flow-controlled vent (1), oxidation and reduction furnaces (2), water trap (3), six-port Valco valve (4), flow-controlled vent (5), packed-column trap (6), and Carbon PLOT capillary column (7).

samples. To our knowledge, the only system with comparable sample-size requirements to the nano-EA system is the moving-wire interface. This interface requires only 0.75 nmol of C for comparable precision (1.0 ‰ 2σ), but samples must be soluble in water or organic solvent and must not be volatile or decompose at temperatures used to dry the solvent (50−150 °C).[4] Advantages to the nano-EA approach include the ability to measure both C and N isotopes, a wide range of sample materials and matrixes, and its basis on commercially available equipment commonly found in stable isotope laboratories. We also fully describe the calculations and treatment of uncertainty necessary for precise and accurate analyses. Finally, we suggest procedures for measuring samples and standards to simultaneously minimize sample requirements and analytical uncertainties.

EXPERIMENTAL SECTION

Elemental Analyzer. The commercial EA system (ECS 4010, Costech Analytical) consists of an autosampler, reactors that convert the sample C and N to CO_2 and N_2 via combustion and reduction, a water trap, a packed GC column for separation of analyte gases, and a thermal conductivity detector. The "zero-blank" autosampler has a sealed body with a helium purge line, vent valve, and isolation valve (Figure 1). The standard combustion and reduction reactors are quartz tubes (45.4 cm long, 18 mm o.d., 14 mm i.d., 2 mm wall thickness) packed with chromium(III) oxide and silvered cobalt(II, III) oxide and reduced copper wires, respectively. The oxidation reactor is heated to 1020 °C and the reduction reactor to 650 °C. The manufacturer's water trap is a glass tube (11 cm long, 8 mm i.d., plastic end-fittings with Teflon/rubber O-rings) packed with magnesium perchlorate. CO_2 and N_2 are separated on a packed GC column maintained at 50 °C during typical EA analyses.

We extensively tested the commercial EA system and made several modifications to reduce the procedural blank. These modifications (described below) include autosampler evacuation and purge lines, narrower quartz reactors,[5] and a lower volume

water trap. The packed GC column and thermal conductivity detector were removed from the flow path, and the effluent from the EA is transferred directly to the custom trapping system through 1/16 in. stainless steel tubing.

Trapping System. The trapping system includes a cryogenic/heated trap made from a deactivated stainless-steel chromatography column ("silicosteel") packed with silica gel (0.75 mm i.d., 0.18 m length, PC3645 Restek Corporation), six-way Valco valve (p/n C6WE, VICI Valco Instruments), low-flow helium supply, and capillary column (Carbon PLOT, 30 m length, 0.320 mm i.d., 1.50 μm thick stationary phase, JW Scientific) (Figure 1). The valve switches between two positions selecting both the input and output of the cryogenic trap. The gas flow either enters the trap from the EA and exits through a flow-controlled vent (trap position) or enters from the low-flow helium source and exits to the capillary column and ultimately the mass spectrometer (purge position).

Isotope Ratio Mass Spectrometer. The isotopic ratio of gases from the EA and trapping system were measured on a Thermo-Finnigan Delta Plus IRMS. The EA or trapping system carrier stream was sent to a ConFlo III interface[1] that splits the stream, sending 0.2 cm^3 min^{-1} to the mass spectrometer. This interface is also used to inject pulses of reference CO_2 and N_2 gases into the carrier stream for standardizing the isotopic measurements and optionally dilute the EA carrier stream with additional helium flow. Chromatograms were integrated and isotopic ratios calculated using the Isodat software package (v1.42).

Measurement Procedure. Samples are placed or pipetted into precleaned silver foil capsules. Solvent is allowed to evaporate and the capsules are sealed by folding them with tweezers. Before analysis, the trap is heated to 120 °C with resistive heating tape and the valve is set to the "purge" position (Figure 1). The EA system is then started, initiating oxygen flow into the combustion reactor and signaling the autosampler to drop a sample. The sample C and N are converted to CO_2 and N_2 gases in the EA reactors, pass through the water trap, and exit the EA. About 10 s before these gases enter the trapping system, the heating tape power supply is switched off, and the trap is plunged into liquid nitrogen to cool to −196 °C. At a time 5 s before the analyte gases reach the valve, the valve is turned to the "trap" position and the sample gases are cryogenically removed from the EA carrier stream onto the silica gel column. After all of the analyte gases have been trapped, the valve is switched to the "purge" position and the trap is removed from the liquid nitrogen and heated to 120 °C with the resistive heating tape. At this point, the sample gases evaporate into the low-flow helium stream and are separated by the Carbon-PLOT column into N_2 and CO_2 peaks before entering the ConFlo III gas interface. The separation between these peaks is long enough that the N_2 peak is recorded at m/z 28 and 29 by the mass spectrometer, the electromagnet "jumps" to the CO_2 magnet setting, and the CO_2 peak is then recorded at m/z 44, 45, and 46 (Figure 2). When measuring C and N isotopes on the same sample, the CO_2 peak often saturates the IRMS detectors because many analytes have C/N ratios $\gg$ 1. This difficulty is overcome by optionally diluting the CO_2 with helium in the ConFlo III, upstream of the transfer capillary to the mass spectrometer.

(4) Sessions, A. L.; Sylva, S. P.; Hayes, J. M. *Anal. Chem.* **2005**, *77*, 6519–6527.

(5) Carman, K., R.; Fry, B. *Mar. Ecol.: Prog. Ser.* **2002**, *240*, DOI: 10.3354/meps240085.
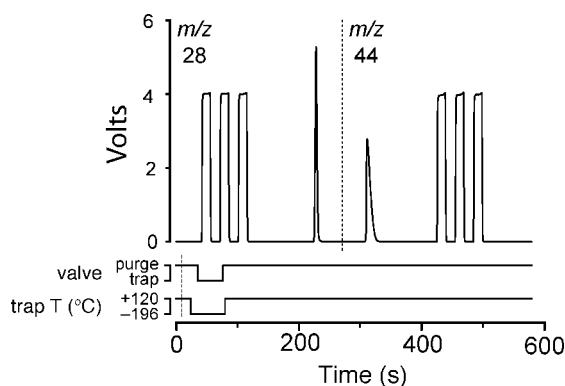
Figure 2. A typical nano-EA chromatogram illustrated by the N_2 (m/z 28) and CO_2 (m/z 44) ion currents for a caffeine standard. Square peaks at the beginning and end are pulses of N_2 and CO_2 laboratory gas, respectively, used to reference the sample isotopic composition. The dashed line at the left shows when the sample drops into the EA reactor.

We reduce the procedural blank by minimizing the duration of cryogenic trapping while assuring quantitative recovery of the sample gas. The trapping interval is determined using the peak beginning and end times observed on the EA thermal conductivity detector and is measured relative to the time the sample is dropped into the oxidation furnace. Using the He flow rate and tubing volumes, and considering changes in flow rates because of valve position and trap temperature (Figure 2), we calculate the timing and duration of the analyte peak in the trapping system. The thermal conductivity detector is subsequently removed from the flow path to reduce peak broadening and the timing adjusted by the reduction in retention time measured at the IRMS.

CALCULATIONS

Isotope results are reported using the δ notation:

$$\delta = (R - 1) \tag{1}$$

where R is the standardized isotopic ratio and $(^{13}C/^{12}C)_s/(^{13}C/^{12}C)_{ref}$ or $(^{15}N/^{14}N)_s/(^{15}N/^{14}N)_{ref}$ and subscripts indicate the sample or isotopic reference. (In the following equations, all δ values are expressed in units of parts-per-thousand, ‰, and therefore refer to the right-hand side of eq 1 multiplied by 10^3.) The sample isotopic composition is measured directly relative to either the CO_2 or N_2 laboratory reference gas ($\delta_{S_{Ref}}$), and the composition of the sample relative to the internationally recognized $\delta^{13}C$ and $\delta^{15}N$ scales, VPDB and AIR, is calculated by

$$\delta_{S_{AIR}} = \delta_{S_{Ref}} + \delta_{Ref_{AIR}} + 10^{-3} \delta_{S_{Ref}} \delta_{Ref_{AIR}} \tag{2}$$

The reference gas value on the international scales is determined from isotopic standards with known composition ($\delta_{Std_{AIR}}$) that are analyzed identically to samples:

$$\delta_{Ref_{AIR}} = (\delta_{Std_{AIR}} - \delta_{Std_{Ref}})/(1 + 10^{-3} \delta_{Std_{Ref}}) \tag{3}$$

In a single measurement, the fractional abundance of the rare isotope, $F_M = {}^{13}C/({}^{12}C + {}^{13}C)$ or ${}^{15}N/{}^{14}N + {}^{15}N$, reflects the

amount-weighted fractional abundance of the sample (F_S) plus procedural blank (F_B)

$$F_M = \frac{A_S F_S + A_B F_B}{A_M} \tag{4}$$

where the measured sample amount A_M equals $A_S + A_B$. The fractional abundances in eq 4 can be approximated by isotopic ratios (and thus δ values) without large errors when isotopic differences are small (as is true for C and N).[6] Accordingly, eq 4 can be written in a linear form that describes a mixing line between the procedural blank ($1/A_B$, δ_B) and the isotopic composition of the sample gas ($\lim_{A_S \to \infty} 1/A_M$, δ_S):[7]

$$\delta_M = \delta_S + \frac{A_B(\delta_B - \delta_S)}{A_M} \tag{5}$$

A single measurement can be corrected for the blank contribution using experimentally determined mean values for A_B and δ_B:

$$\delta_C = \frac{A_M \delta_M - \bar{A}_B \bar{\delta}_B}{A_M - \bar{A}_B} \tag{6}$$

Alternatively, the y-intercept from a weighted least-squares fit of eq 5 to a suite of sample replicates that vary in size allows calculation of the blank-corrected isotopic composition of the sample. It is important to note that both A_M and δ_M are subject to error and the misfit in both x and y should be minimized. In practice, unweighted regression yields nearly identical coefficients though uncertainties are more variable.

Blank Composition and Variability. Two approaches are possible to calculate the size, composition, and variability of the procedural blank (A_B, δ_B, σ_{A_B}, σ_{δ_B}). First, repeat analyses of the blank can directly yield these parameters if the blank is large enough to measure accurately. Second, the intersection of the regression solution to eq 5 for two samples or standards (m_1, δ_1, m_2, δ_2) can provide A_B and δ_B if the blank is too small to measure directly:

$$\bar{A}_B = \frac{m_1 - m_2}{\delta_2 - \delta_1} \tag{7a}$$

$$\bar{\delta}_B = \frac{m_2 \delta_1 - m_1 \delta_2}{m_2 - m_1} \tag{7b}$$

where δ and m are the intercept and slope from regression. Values for σ_{A_B} and σ_{δ_B} are then calculated from the uncertainty in the slope and intercept:[8]

$$\sigma_{A_B}{}^2 = \frac{1}{D^2}\left(\sigma_{m_1}{}^2 + \sigma_{m_2}{}^2 + \frac{M^2}{D^2}(\sigma_{\delta_1}{}^2 + \sigma_{\delta_2}{}^2)\right) \tag{8a}$$

(6) Sessions, A. L.; Hayes, J. M. *Geochim. Cosmochim. Acta* **2005**, *69*, 593–597.
(7) Keeling, C. D. *Geochim. Cosmochim. Acta* **1958**, *13*, 322.
(8) Gelwicks, J. T.; Hayes, J. M. *Anal. Chem.* **1990**, *62*, 535–539.

$$\sigma_{\delta_B}{}^2 = \frac{1}{M^2}\left(\frac{D^2}{M^2}(m_2{}^2\sigma_{m_1}{}^2 + m_1{}^2\sigma_{m_2}{}^2) + m_2{}^2\sigma_{\delta_1}{}^2 + m_1{}^2\sigma_{\delta_2}{}^2\right)$$

$$(8b)$$

where $M = m_1 - m_2$ and $D = \delta_1 - \delta_2$. Equation 7 and eq 8 can yield estimates for the blank composition and variability; however, the accuracy is often less than produced by direct measurement. Additionally, the uncertainty calculated by eq 8 often does not reflect the true variability of the blank and should not be used to calculate the uncertainty in the measured or blank-corrected sample values (see below). If the blank is small, it is possible to increase the blank peak height by decreasing the low-flow helium flow rate and measure the blank directly, with proper consideration of the transmission efficiency (discussed below). In all cases direct measurements of the blank are preferred because they provide estimates for $\bar{A}_B$, $\bar{\delta}_B$, σ_{A_B}, and σ_{δ_B} with more accurate uncertainties than those from regression.

Uncertainty in Blank-Corrected Values. Uncertainty in the blank-corrected sample value (δ_C) depends upon how the correction was accomplished. If the blank contribution is removed from each measurement with eq 6, then

$$\sigma_{\delta_C}{}^2 = \left(\frac{\partial\delta_C}{\partial A_B}\right)^2\sigma_{A_B}{}^2 + \left(\frac{\partial\delta_C}{\partial\delta_B}\right)^2\sigma_{\delta_B}{}^2 + \left(\frac{\partial\delta_C}{\partial a}\right)^2\sigma_a{}^2 + \left(\frac{\partial\delta_C}{\partial\bar{A}_B}\right)^2\sigma_{\bar{A}_B}{}^2 +$$
$$\left(\frac{\partial\delta_C}{\partial\bar{\delta}_B}\right)^2\sigma_{\bar{\delta}_B}{}^2 \quad (9a)$$

where σ_a is the analytical uncertainty in the isotopic measurement that includes variability from the EA combustion/reduction chemistry and IRMS measurement (determined from conventional EA analyses: ± 0.08 ‰ for N and ±0.03 ‰ for C). When $\bar{A}_B$ and $\bar{\delta}_B$ are directly measured, $\sigma_{\bar{A}_B} \ll \sigma_{A_B}$, $\sigma_{\bar{\delta}_B} \ll \sigma_{\delta_B}$, the uncertainty in $\bar{A}_B$ and $\bar{\delta}_B$ can be ignored and eq 9a becomes

$$\sigma_{\delta_C}{}^2 = \left(\frac{\delta_M}{A_M - \bar{A}_B} + \frac{\delta_B - \delta_C}{A_M} + \frac{\bar{A}_B\bar{\delta}_B - A_M\delta_M}{(A_M - \bar{A}_B)^2}\right)^2\sigma_{A_B}{}^2 +$$
$$\left(\frac{A_B}{A_M - \bar{A}_B}\right)^2\sigma_{\delta_B}{}^2 - \left(\frac{A_M}{A_M - \bar{A}_B}\right)^2\sigma_a{}^2 \quad (9b)$$

(If $\bar{A}_B$ and $\bar{\delta}_B$ are determined by regression, their uncertainty is much larger and their partial differential terms should be included.) If δ_C is calculated by regression, then the uncertainty in the intercept value gives σ_{δ_C}.

Once δ_C and σ_{δ_C} are known, eqs 2 and 3 are used to calculate the sample value on the VPDB or AIR scales, propagating the uncertainties in δ_C and δ_{Ref}:

$$\sigma_{\delta_{C_{AIR}}}{}^2 = \left(1 + 10^{-3}\delta_{Ref_{AIR}}\right)^2\sigma_{\delta_{C_{Ref}}}{}^2 + \left(\frac{1 + 10^{-3}\delta_{C_{Ref}}}{\left(1 + 10^{-3}\delta_{Std_{Ref}}\right)^2}\right)\sigma_{\delta_{Std_{Ref}}}{}^2 +$$
$$\left(\frac{1 + 10^{-3}\delta_{C_{Ref}}}{1 + 10^{-3}\delta_{Std_{Ref}}}\right)^2\sigma_{\delta_{Std_{AIR}}}{}^2 \quad (10)$$

RESULTS AND DISCUSSION

Blank Reduction. The blank in the nano-EA system is of two types. The first includes N_2 or CO_2 constantly present in the

He carrier stream exiting the EA. In conventional EA analyses, this type of background is readily accounted for by accurate baseline determinations. In contrast, the nano-EA system is sensitive to any background in the carrier stream because this background is trapped along with the sample. Prior to modifying the EA system, we found no detectable carbon dioxide blank associated with the carrier gas stream and a nitrogen blank of ~150 nmol of N. We have reduced this N background to 83 nmol, both by removing its sources and minimizing the trapping time for the sample peak. (1) Water trap: The manufacturer's water trap was replaced with a borosilicate glass tube (6.35 mm o.d., 3.81 mm i.d., 150 mm length) packed with magnesium perchlorate and installed with Swagelok stainless steel end fittings and Teflon ferrules. This modification reduced the nitrogen blank from atmospheric leaks and also decreased the trap volume by ~70%, decreasing peak broadening, trapping time, and further reducing the blank size. The N blank size decreased by 43.5 nmol (29%) from this replacement. (2) Quartz reactors: Replacement of the 14 mm i.d. quartz reactors with custom-made 10 mm i.d. reactors decreased the furnace volume by 50%, reducing the volume of He carrier gas required to transmit the sample gases through the EA to the cryogenic trap. The reduced He volume proportionally decreased the volume of background N_2 passing through the cold trap during the trapping period, reducing the N blank by 19.5 nmol (13%). These narrow-bore oxidation and reduction reactor tubes are constructed by centering a small diameter quartz tube (14 mm o.d., 10 mm i.d., 45.4 cm length) with flared ends inside a second quartz tube (18 mm o.d., 16 mm id, 45.4 cm length) and fusing the tube ends together. A ~3 mm hole drilled in the outer tube 3 cm from one end allows gas trapped between the tubes to escape during heating. (3) Autosampler: Small leaks in the body of the autosampler that contributed to an increasing N_2 blank during a run were eliminated by allowing a small amount of the He carrier gas (6.0 cm³ min⁻¹, 4.6% of the total flow) to bleed out of the autosampler body through a valve and flow controller. This modification constantly purges the autosampler–EA connection and prevents the blank value from increasing over the course of a run.

Tests of the helium carrier gas, O_2 gas, and oxidation and reduction reagents indicate they are not the source of the remaining N background. We recently identified several small leaks in the EA fittings that further reduced the N blank to ~23 nmol and lowered the variations in the blank size proportionally. The variability in the isotopic composition of the blank did not change. These improvements have decreased the minimum sample size for N to <10 nmol (C measurements were not affected); however, the standards and samples reported in this paper were measured with the larger N blank, and for consistency we describe precision and accuracy of the larger-blank system.

The second source of background is intimately associated with the sample, sample container, and the valve switching that occurs when the sample is introduced to the combustion furnace. (1) Atmospheric gases: Atmospheric N_2 and CO_2 trapped in the sample container can be a significant blank source. We modified the Costech zero-blank autosampler with a valve attached to a vacuum line and evacuated the autosampler
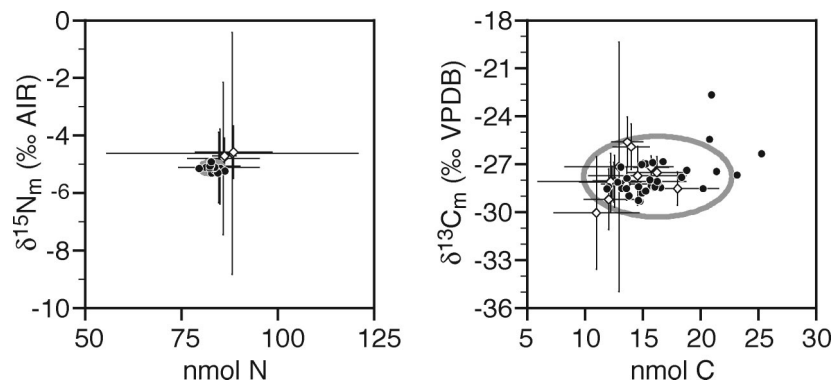
Figure 3. Blank size, composition, and uncertainty determined by measurement and the intersection of lines fitted to a dilution series of standards or samples. Circles indicate actual blank measurements, and gray ellipses contain the 2σ range for these blank values. Diamonds and error bars denote blank composition $\pm\ 2\sigma$ determined by the intersection of lines fit to the data in Figure 4.
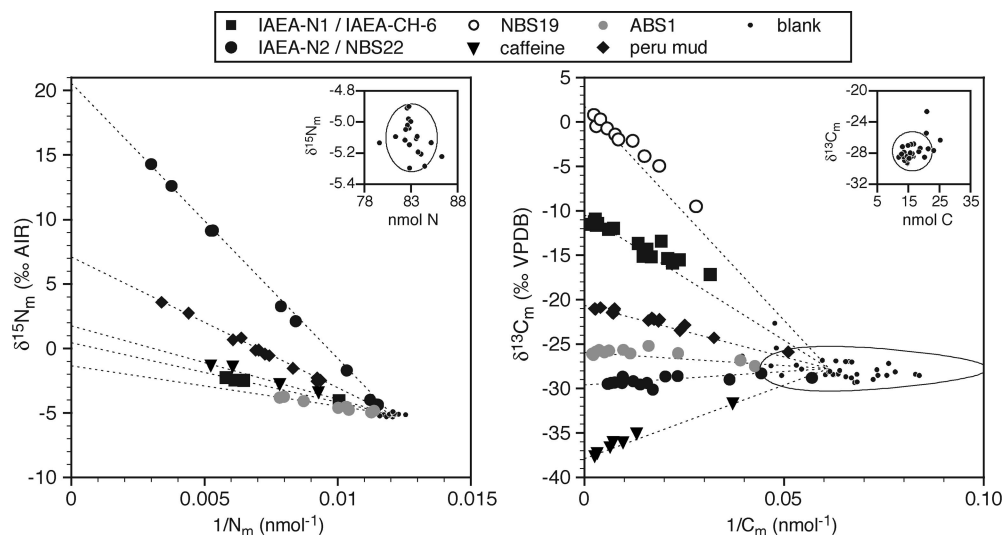
Figure 4. Measured blank and standard isotopic compositions versus the inverse of the amount measured. Dashed lines illustrate mixing between the average blank and expected sample end members. Ellipses contain the 2σ range for blank values, and the inset shows blank composition versus size.

volume and purged it with He several times before analyses (Mike Lott, University of Utah, personal communication, 2004). This technique virtually eliminates atmospheric contamination in the sample containers. (2) Sample containers: Foil sample "boats" contributed significant carbon and a small amount of nitrogen to the blank. We observed large differences in the size and variability of the blank depending upon the material (silver or tin), supplier, and our cleaning procedure for the boats. Experiments with ashing, rinsing, and leaching revealed the lowest blanks occurred with 4 mm × 6 mm pressed silver capsules (CE-Elantech) ashed at 450 °C for 8 h. Ashing completely eliminated the nitrogen blank from the foil and decreased the carbon blank by ~50 nmol. However, the carbon contained within the silver foil is still the largest contributor to the blank during $\delta^{13}C$ measurements. Variability of the amount and isotopic composition of C in tin boats was smaller than in the silver boats and we have begun using solvent-rinsed tin boats for C-only analyses.

Blank Size and Composition. Repeated measurements of the analytical blank are shown in Figure 3. The nitrogen blank has a nearly uniform composition and size ($\delta_B = -5.11 \pm 0.11$ ‰ AIR, $A_B = 83.1 \pm 1.4$ nmol of N, $\pm 1\sigma$) and is probably derived from diffusion-dominated leaks in the numerous fittings of the

elemental analyzer. The small deviations in size and isotopic composition of the N blank allow accurate measurements of samples much smaller than the size of the blank. In contrast, the size of the carbon blank is much smaller than that of nitrogen but the larger variability prevents accurate measurements of very small samples ($\delta_B = -27.76 \pm 1.26$ ‰ VPDB, $A_B = 16.3 \pm 3.2$ nmol of C, $\pm 1\sigma$). The isotopic composition of the blank carbon suggests contamination of the silver boats with small amounts of hydrocarbons. However, our cleaning and ashing procedure is unable to remove this carbon, and we infer it is pervasive in the silver foil and protected from oxidation. Isotopic measurements on a single foil boat split into equal halves differed by 2.8 ‰, indicating that small-scale heterogeneity is responsible for the large variability of the carbon blank.

We tested regression-based determination of the blank using the intersection of lines fitted to sample replicates (Figure 3). The values produced by this method were reasonably similar to the measured carbon blank but different from the nitrogen blank. Importantly, the uncertainties in the intersection-determined blank size and composition (calculated from the uncertainties in the fitting parameters) do not reflect the actual distribution of blank size and compositions determined by direct measurement of the blank. Further, calculated estimates of uncertainty exhibit greater

Table 1. Nitrogen and Carbon Isotopic Compositions of International and Laboratory Standards (‰ AIR and VPDB, Respectively)[a]

	accepted		conventional EA			nano EA					nano EA (intercept)			
	δ	$\pm1\sigma$	δ	$\pm1\sigma$	n	δ	$\pm1\sigma$	n	Δ_{C-N}	$\pm1\sigma$	δ	$\pm1\sigma$	Δ_{C-N}	$\pm1\sigma$
						Nitrogen								
IAEA-N1[b]	0.4	0.2	0.43	0.11	7	0.43	0.20	4		0.23	0.43	0.13		0.17
IAEA-N2	20.3	0.2	20.66	0.16	21	20.50	0.55	9	−0.16	0.58	21.01	0.15	+0.35	0.22
caffeine			1.75	0.11	11	1.79	0.47	4	+0.04	0.48	1.93	0.52	+0.18	0.53
peru mud			7.31	0.15	8	6.95	0.35	12	−0.36	0.38	7.42	0.17	+0.11	0.23
ABS1			−1.08	0.23	5	−1.37	0.44	8	−0.29	0.50	−0.93	0.26	+0.15	0.35
						Carbon								
IAEA-CH-6[b]	−10.449	0.033	−10.45	0.10	16	−10.45	0.38	16		0.39	−10.45	0.26		0.28
NBS-19	1.95	c	1.89	0.13	6	1.82	0.80	10	−0.07	0.81	1.86	0.30	−0.03	0.32
NBS-22	−30.031	0.043	−30.03	0.07	4	−29.57	0.38	14	+0.46	0.38	−29.12	0.19	+0.91	0.20
caffeine			−37.97	0.15	11	−37.89	0.33	7	+0.08	0.36	−37.35	0.18	+0.62	0.23
peru mud			−20.66	0.11	9	−20.61	0.24	17	+0.05	0.26	−20.22	0.10	+0.44	0.15
ABS-1			−25.97	0.08	3	−25.90	0.28	12	+0.07	0.29	−25.31	0.17	+0.66	0.19

[a] N1 and N2 are ammonium sulfate standards, CH-6, NBS-19 and NBS-22 are sucrose, oil, and calcium carbonate, respectively, caffeine is reagent grade (Aldrich, lot no. 09905EN), and Peru mud and ABS1 (Archean Black Shale) are decalcified and homogenized marine sediments used as PSU laboratory standards. Nano-EA mean and standard deviations are $1/\sigma^2$-weighted while conventional EA statistics are unweighted. Nano-EA (intercept) values are calculated from least-squares fits of eq 5 to the data in Figure 4. No error in both x- and y-values was assumed, and uncertainty in the fitting parameters is derived from the dispersion of the data. All EA deviations characterize the internal precision and do not include uncertainties in the reference material values used to calibrate the isotope scale. Replicates ranged in size from 3.7 to 250 nmol although 90% were less than 110 nmol. Δ_{C-N} is the difference between conventional and nano-EA results. [b] Calibration standard. [c] Definition of VPDB scale.

variability relative to those determined by direct measurements of the blank (illustrated by the range of error bar sizes in Figure 3). As a consequence, use of the line-fitted blank size and composition for blank correction yields poorer accuracy and uncertain precision compared to directly measured blank values. These data emphasize the importance of measuring the blank directly whenever possible.

Accuracy. We evaluated the accuracy of the nano-EA measurements using international and Pennsylvania State University (PSU) laboratory isotopic standards analyzed by nano-EA and conventional EA (Figure 4). A range of replicate sizes were analyzed and each measurement was corrected for the blank using eq 6. The confidence interval (internal precision) for each measurement was calculated using eq 9a. Data from replicates were averaged and compared with conventional EA measurements and accepted values for the international standards.

The $\delta^{15}N$ and $\delta^{13}C$ of nano-EA and conventional-EA measurements are nearly identical and their differences do not differ significantly from zero (Table 1). The differences between nano-EA-determined and internationally accepted values for standards are similarly small and well within the external and smaller internal precision of the averages. These small differences give confidence that nano-EA measurements supply the same isotopic information as conventional EA analyses and correctly reproduce the AIR and VPDB scales. The largest difference occurred for the NBS-22 oil (+0.45 ‰ $\delta^{13}C$) and probably reflects a combination of chance (this difference is only 1.2 times the standard deviation of the mean) and our calibration to the VPDB scale. Recently, new guidelines have changed the scale for reporting of $\delta^{13}C$ values to include a second standard (L-SVEC, −46.6 ‰) to anchor the scale.[9] As a result, consensus values for NBS-22 and other standards shifted, with most of the change due to the anchoring procedure and thus increasing in magnitude with an increasing isotopic difference from NBS-19. We

(9) Coplen, T. B.; Brand, W. A.; Gehre, M.; Groning, M.; Meijer, H. A. J.; Toman, B.; Verkouteren, R. M. *Anal. Chem.* **2006**, *78*, 2439–2441.

anchored our $\delta^{13}C$ scale with IAEA-CH-6 (−10.45‰) because we found smaller variability in replicate analyses compared to NBS-19. Anchoring and scaling our $\delta^{13}C$ values with NBS-19 and IAEA-CH-6 results in −29.77 ‰ for NBS-22 by nano-EA (+0.26 relative to the consensus value) and −30.12 ‰ for conventional EA measurements. Both values are well within internal measurement uncertainties. Regardless of the source, the difference between the measured and expected values for NBS-22 are relatively small and do not change the conclusions of the paper. In the future, nano-EA measurement of NBS-19 and L-SVEC would decrease this uncertainty.

In addition to blank-correction of individual measurements, we also tested blank correction using the intercept of lines fitted to sample data on a $1/A_M$ versus δ_M plot (Figure 4; Table 1). These values for nitrogen were comparable to the individual corrections applied above while the carbon values were generally less accurate than the individual blank correction averages. The differences for carbon may reflect the larger variability in the blank and its effect upon the fitting parameters (see below). (Note that this approach is distinct from determination of blank size and composition by the intersection of fitted lines and subsequent blank correction with these values.)

Precision. The theoretical precision of individual measurements predicted by eq 9a was tested using the distribution of deviates from all replicates of standards and samples measured by nano-EA. The deviates (measured minus mean) as a function of sample size generally fall within the 2σ ranges predicted by theory (Figure 5, lower panels). These ranges also depend upon the isotopic difference between sample and blank; therefore, a more rigorous test is provided by the distribution of deviates normalized to the standard deviation predicted by theory for each measurement (Figure 5, upper panels). The frequency distributions of these normalized deviates are similar to that of a Gaussian indicating the theoretical precision calculated from eq 9a closely estimates the internal precision of an individual measurement. The slightly broader distribution of deviates for carbon measurements
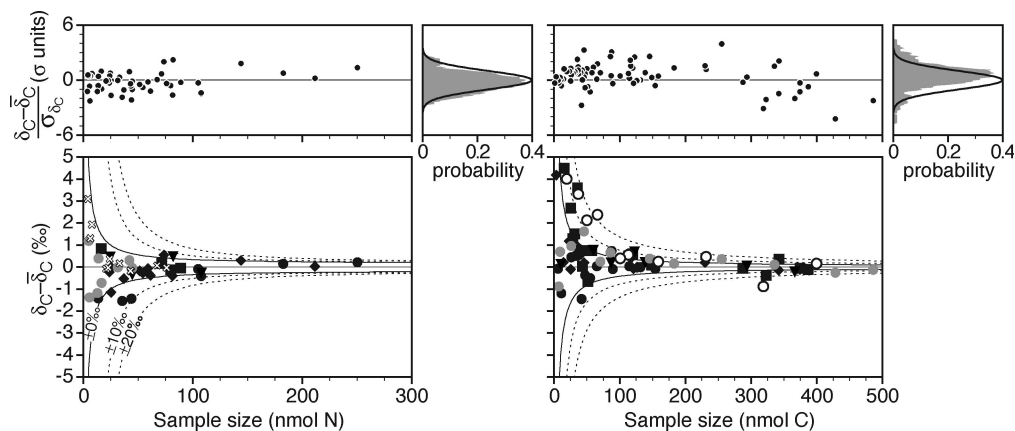
Figure 5. Comparison between measured variability of blank-corrected sample values and that predicted from theory. Bottom panels show the differences of individual blank-corrected values from the $1/\sigma^2$-weighted averages for each standard and 2σ confidence intervals predicted from theory (symbols as in Figure 4). Numbers on solid and dashed lines indicate the difference between sample and blank isotopic compositions used to calculate the confidence range. The upper panels plot the differences in the lower panels normalized by the standard deviation calculated individually for each measurement (eq 9a). The histograms illustrate the frequency distribution of these values compared to that expected for a Gaussian distribution of zero mean and unit standard deviation.

is chiefly driven by the broader range of those from larger samples (which have small predicted standard deviations). Excluding deviates for large samples results in a distribution that is closer to normal but still slightly broader. Factors not included in eq 9a such as sample heterogeneity and biases inherent in the blank correction (see below) may contribute to the broader observed distribution. However, the similarity of the observed and theoretical distributions of the normalized deviates indicates that the values calculated from eq 9a provide an accurate measure of the internal precision.

In addition to the checks described above, we tested the blank-correction, line fitting, and uncertainty calculations with Monte-Carlo techniques. Synthetic data sets were generated using randomly sampled blank size, composition, analytical uncertainties, and blank-corrected sample values and uncertainties were determined for each data set ($n = 100\,000$). The distribution across all simulations of the blank-corrected sample values and the uncertainties calculated for each simulated data set were examined. Comparison of these two distributions allows us to evaluate whether the analytical uncertainties calculated from a single data set can provide an accurate estimate of the true uncertainty in the blank-corrected sample values.

Simulations where a single measurement is blank-corrected using known blank size, composition, and variability (eq 6) documented a subtle but important effect on the mean and distribution of the blank-corrected isotopic composition of the sample (δ_C) that depends upon the isotopic difference between the sample and blank. With greater isotopic differences, the distribution of δ_C becomes skewed, resulting in a longer tail away from the blank composition and a systematic bias in the mean δ_C away from the blank composition. This bias is a direct consequence of the inverse transformation of a Gaussian distribution. For the inverse of measured blank amounts ($1/A_B$), negative deviations from the average blank size are farther from the average than positive deviations (Figure 4), and this skewness is imparted to the measured sample values. The blank correction uses a single average value for the blank size and composition ($\bar{A}_B$, $\bar{\delta}_B$) which does not adjust for this skewness;
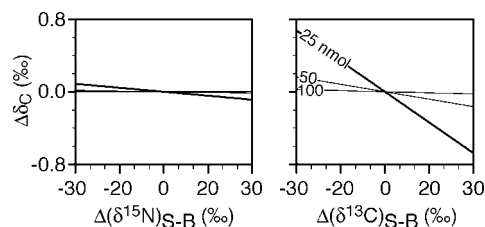
Figure 6. The mean minus expected blank-corrected sample value (from Monte Carlo simulations) as a function of the isotopic difference between the sample and procedural blank shown for different sample sizes.

therefore, the skewed distribution of measured values is translated directly to the mean blank-corrected sample values (Figure 6).

This effect may be significant for small samples when the blank is quite variable (as is the case for C in the PSU nano-EA system). NBS-19 has the largest isotopic difference from the blank, and we observed a trend toward more positive blank-corrected NBS-19 values as sample size decreased. However, these deviations cannot conclusively be attributed to this effect because they are much larger than predicted (+3.9 ‰ observed vs +0.9 ‰ predicted for a 20 nmol replicate) and fall well within the 1σ precision for these measurements. Although not directly detected, it is possible that some of the variability in the normalized deviates (Figure 5) reflects this effect.

The skewed distribution of measured sample values resulting from the inverse transformation of blank size also imparts a systematic bias to the slope and intercept of regression lines fit to $1/A_M$ versus δ_M data. The greater skewness present in smaller sample sizes will bias the intercept toward the isotopic composition of the blank, while the slope will be systematically closer to zero. When the intercept of the regression lines is used for blank correction, the blank-corrected isotopic value will be systematically offset toward the blank composition and the range of blank-corrected isotope values will be reduced. Similarly, when the size and composition of the blank are determined by the intersection of lines fitted to sample replicates, the size of the blank will be underestimated and

the isotopic composition of the blank will be offset from the true value. This underestimation may be responsible for the smaller size for the carbon blank calculated from the intersection of regression lines compared to the size determined by direct measurement of the blank (Figure 3).

Maximum Theoretical Precision and System Performance. The maximum attainable precision in any isotope measurement is given by the shot-noise limit (SNL).[2] At this limit, the ion beam itself is the only source of noise and the variance in the number of ions detected is equal to the number of detected ions ($\sigma_N^2 = N$). The SNL is expressed as[2]

$$\sigma_\delta{}^2 = \frac{2 \times 10^6 (1+R)^2}{E(m/n)x N_A R} \tag{11}$$

where R is the absolute ratio of the ion beams used to calculate isotope ratios (for CO_2, $^{45}i/^{44}i \approx 0.0112$ and for N_2, $^{29}i/^{28}i \approx 0.00074$), E is the ionization efficiency of the mass spectrometer (for our system $\sim$0.0008 CO_2^+/CO_2 and $\sim$0.0004 N_2^+/N_2), m is the moles of sample plus blank introduced to the EA, n is the number of molecules per atom of analyte ($n_{N_2} = 0.5$, $n_{CO_2} = 1$), x is the transmission efficiency (moles of sample introduced to the EA/mol of sample introduced to the MS),[4] and N_A is Avogadro's number (6.02×10^{23}). In the nano-EA system, the ratio between peak area (A) and m is $\sim$1.05 V s nmol of C^{-1} and $\sim$0.115 V s nmol of N^{-1}. The transmission efficiency can be written in terms of this ratio as

$$x = \frac{A}{m} \frac{1}{R_f q_e N_A E n} \tag{12}$$

where q_e is the electronic charge (1.6×10^{-19} C) and R_f is the value for the feedback resistance of the mass-28 or mass-44 electrometer (3×10^8 Ω). The value for x_N is 0.020 while that of x_C is 0.045. The ratio x_N/x_C is 0.44, almost exactly reflecting the ratio of the inverse low-flow He flow rates during N and C analyses (8.6 and 3.7 cm^3 min^{-1}) of 0.45. These flow rates and transfer efficiencies indicate a flow of 0.17 cm^3 min^{-1} through the capillary leak to the MS source and equal trapping efficiencies for CO_2 and N_2. Using these values for x_N and x_C in eq 11, the 2σ SNL for a nano-EA measurement on 41 nmol of C is 0.024 ‰ and on 25 nmol of N is 0.065 ‰. The corresponding 2σ blank-corrected precision calculated from eq 9a is 1.0 ‰ for C and N, 41 and 15 times larger than the SNL, respectively. This calculation indicates significant room for improvement of nano-EA precision, principally through reduction in the blank size and variability. For C analyses this might be accomplished with a supplier or cleaning procedure for the sample boats that reduces the amount of carbon. Nitrogen analyses could benefit from further elimination of atmospheric leaks in the EA by careful testing and modification of fittings and tubing. The size of the nitrogen blank could also be reduced by decreasing the peak width and trapping time. This might be achieved by replacing the separate oxidation and reduction reactors with a single, narrow-bore reactor that combines the oxidation and reduction steps. Replacing the chemical water trap with a cryogenic trap of 1/16 in. stainless-steel tubing immersed dry ice/ethanol (−90 °C) might also improve peak shape and reduce trapping times.

Table 2. Carbon and Nitrogen Isotopic Measurements by Nano-EA on Nanomolar Quantities of Pigment Standards[a]

sample	n	N (nmol)	δ^{15}N	±1σ	C (nmol)	δ^{13}C	±1σ
chlorophyll *a*	1	107.1	4.53	0.69	507	−30.32	0.05
	2	126.6	3.97	0.38	778	−30.59	0.04
	3	150.6	4.23	0.27	1103	−30.70	0.04
	4	159.1	4.12	0.24	1278	−30.85	0.04
	wt avg		4.15	0.15		−30.67	0.20
pheophytin *a*	1	6.5	6.80	2.96			
	2	20.8	5.42	0.83			
	3	22.7	5.47	0.76			
	wt avg		5.49	0.34			
pheorbide *a*	1	4.2	10.20	5.47			
	2	7.9	9.03	2.70			
	3	33.1	7.27	0.57			
	4	43.1	6.93	0.43			
	wt avg		7.10	0.51			

[a] Individual measurement uncertainties are calculated with eq 9a, and mean and standard deviations are calculated as in Table 1.

APPLICATIONS

We have analyzed a variety of samples by nano-EA including organic compounds, inorganic salts, cell biomass, and marine sediments. Many materials have high C/N ratios, and we are able to easily measure δ^{13}C values on most of the samples we analyze for δ^{15}N. Our impetus for developing the nano-EA system was the ability to analyze individual compounds isolated from complex matrixes by analytical HPLC. Recent advances in pigment analysis by quaternary gradient HPLC have improved chromatographic peak separation,[10] and we are now able analyze the isotopic composition of abundant pigment molecules in triplicate from a single HPLC separation. Furthermore, by reducing the sample size requirements of EA-IRMS, we are able to make a single N measurement on less-abundant pigment molecules that were previously inaccessible for stable isotope analyses. An illustration of this application is shown with simultaneous δ^{15}N and δ^{13}C measurements on a chlorophyll *a* standard and δ^{15}N measurements on small amounts of chlorophyll derivatives used to evaluate HPLC purification (Table 2). We have also found the system useful for δ^{15}N measurements on low-N materials, such as clay-bound N in marine sediments, that would require several grams of sample for a conventional EA analyses. The nano-EA system could easily measure the isotopic compositions of a variety of biochemicals such as sugars, proteins, and amino acids separated by HPLC or other methods.

CONCLUSIONS

Our experience with nano-EA measurements on standard and sample materials has led us to adopt several conventions that maximize precision and accuracy. First, a comprehensive treatment of errors demonstrates that the procedural blank should be directly measured instead of calculated by regression, and that blank-corrected sample values should be calculated individually using eq 6 rather than by regression. Second, the analytical formula for internal precision of blank-corrected sample values

(10) Airs, R. L.; Atkinson, J. E.; Keely, B. J. *J. Chromatogr., A* **2001**, *917*, 167.

(eq 9a) is adequate when the isotopic difference between the blank and samples ($\Delta(\delta_{S-B})$) is not large. Likewise, the mean and standard deviation calculated with $1/\sigma^2$-weighted averages of replicate measurements provide an accurate estimate for the true value when $\Delta(\delta_{S-B})$ is small. However, as $\Delta(\delta_{S-B})$ increases, the $1/\sigma^2$-weighted average is a biased estimator of the true value because the distribution of blank-corrected sample values is skewed. The blank-corrected mean and uncertainty for these samples can be calculated using techniques that account for this skewed distribution.